Revision# 2

FURTHER INVESTIGATION OF THE INITIAL FISSION-TRACK LENGTH AND GEOMETRY FACTOR IN APATITE FISSION-TRACK THERMOCHRONOLOGY

Cleber J. Soares, [1,2*] Sandro Guedes, [2] Carlos A. Tello, [3] Arnaldo L. Lixandrão Filho, [2] Ana M. Osório, [3] Igor Alencar, [2] Airton N.C. Dias, [4] Julio Hadler, [2]

[1] Instituto de Geociências e Ciências Exatas-IGCE/UNESP, 13506-900, Rio Claro-SP, Brazil.

[2] Instituto de Física "Gleb Wataghin"-UNICAMP, 13083-859 Campinas-SP, Brazil.

[3] Depto. de Física, Química e Biologia – FCT/UNESP, 19060- 900, Presidente Prudente-SP, Brazil.

[4] Laboratório de Geologia Isotópica-CPGq/UFRGS, 91501-970, Porto Alegre-RS, Brazil.

Abstract. The External Detector Method (EDM) is a widely used technique in Fission Track Thermochronology, FTT, in which two different minerals are concomitantly employed: spontaneous tracks are observed in apatite and induced ones in the muscovite external detector. They show intrinsic differences in detection and etching properties that should be taken into account. In this work, new geometry factor values, *g*, in apatite were obtained by directly measuring the ρ_{ed}/ρ_{is} ratios and independently determined $[GQR]_{\text{ed/is}}$ values through the measurement of projected lengths. Five mounts, two of which were large area prismatic sections and three samples composed of random orientation pieces have been used to determine the *g*-values. A side effect of applying EDM is that the value of the initial confined induced fission track, L_0, is not measured in routine analyses. The L_0-value is an important parameter to quantify with good confidence the degree of annealing of the spontaneous fission tracks in unknown-age samples, and is essential for accurate thermal history modeling. The impact of using arbitrary L_0-values on the inference of

This is a preprint, the final version is subject to change, of the American Mineralogist (MSA)
Cite as Authors (Year) Title. American Mineralogist, in press.
(DOI will not work until issue is live.) DOI: http://dx.doi.org/10.2138/am.2014.4140

sample thermal history is investigated and discussed. The measurement of the L_0-value for each sample to be dated using an extra irradiated apatite mount is proposed. This extra mount can be also used for determining the g value as an extension of the ρ_{ed}/ρ_{is} ratio method. Eight apatite samples from crystalline basement, with grains at random orientation, were used to determine the g-values. The results found are statistically in agreement with the values found for Durango samples measured in prismatic section and also measured at random orientation. There was no observable variation in efficiency regarding crystal orientation, showing that it is relatively safe using non prismatic grains, especially in samples with paucity of grains, as it is the case of most basin samples. Implications for the ζ-calibration and for the calibration of the direct (spectrometer-based) fission-track dating are also discussed.

Keywords: Fission-track termochronology, Geometry factor, ϕ-method, ζ-calibration, Initial fission-track length.

***Correspondence to:** Cleber Jose Soares, Instituto de Geociências e Ciências Exatas-IGCE/UNESP, 13506-900, Rio Claro-SP, Brazil. . **e-mail address:** pccj13@yahoo.com.br

Always consult and cite the final, published document. See http://www.minsocam.org or GeoscienceWorld

1. Introduction

The most used procedure for fission-track dating is the External Detector Method (EDM). In this procedure, spontaneous fission-track density is determined in an apatite internal surface (under 4π geometry) whereas induced fission-track density is determined in a muscovite external-detector (under 2π geometry). Considering the difference between geometries as well as the efficiency of revelation by etching and observation, the geometry factor, *g*, must be taken into account. Although the *g*-value is crucial for fission-track dating, there are only a limited number of studies on it (Gleadow and Lovering, 1977; Green and Durrani, 1978; Iwano and Danhara, 1998; Jonckheere and Van den haute, 2002; Jonckheere, 2003; Enkelmann and Jonckheere, 2003). It has been recommended that only clear, c-axis parallel (prismatic) grains of apatite should be selected for fission-track dating (e.g., Gleadow et al. 2002). However, under certain conditions, in which there is paucity of apatite grains, it may be useful to count tracks also in non-prismatic section grains (e.g., Tello et al. 2003, 2005; Ribeiro et al. 2005; Franco-Magalhães et al. 2010). However, it turns out that the *g*-value for these samples is measured in closely ideal large area single crystals (referred to as extensive surfaces through the rest of this work). Grain surfaces with different orientations present different etching characteristics (Jonckheere and Van den haute, 1996), which may lead to variation in analyst efficiency for counting tracks, in such a way that the value of *g* measured in prismatic section crystals may not reflect the actual observer counting efficiency.

The *g*-value has been regarded as a necessity only for the application of the ϕ-method for the calibration of the neutron dosimetry, i.e., the dating method in which neutron fluence is independently measured by neutron monitors (Jonckheere, 2003; Iunes et al. 2002; Soares et al. submitted). However, as it will be shown below, the ages obtained by ζ-calibration may also be affected because the standard and the unknown age samples do not necessarily have their tracks counted with the same efficiency. Particularly, the automatic counting of fission tracks that has been recently proposed (Gleadow et al. 2009) would benefit much by the measurement of *g*-value for the standard and for the unknown age sample. In this case, the surface characteristics of each sample have a more significant effect on counting efficiency than in the traditional counting.

This study is also useful because, as it will be discussed bellow, the procedures involved in determining the geometry factor yield the efficiency factors needed for FT dating using LA-ICP-MS.

The first goal of this work is to further investigate the geometry factor used to calibrate EDM ages, including samples presenting non-ideal conditions. The geometry factor has been determined using projected length distributions (Dakowski, 1978; Green and Durrani, 1978; Jonckheere and Van den Haute, 1999, 2002; Jonckheere, 2003) and through the measurements of induced track densities in an apatite internal surface. This last experiment demands the irradiation of an extra mount containing pre-annealed apatite grains, along with the EDM mounting, so that the track densities in the EDM muscovite and in the irradiated pre-annealed apatite can be compared.

For these two determinations, Durango apatite crystals were cut to expose extensive prismatic surfaces and also pieces of crushed Durango apatite with random orientations were assembled. In addition, one apatite sample (TF-42) from a gneiss rock from Ilha Bela, São Paulo State, Brazil was also used (Tello et al. 2003, 2005). The TF-42 sample was chosen because presents higher induced fission-track density than the other samples presented here, resulting in a better statistic. In addition, the results of electron microprobe analysis (EMPA) carried out at the Institut für Geowissenschaften, Johannes Gutenberg-Universität Mainz have shown the chlorine content of 0.39±0.02 and fluorine content of 3.35±0.02 (Cl/F ratio ≈0.12±0.006), value similar to that found for Durango apatite with chlorine content of 0.42±0.01 and fluorine content of 3.33±0.06 (Cl/F ratio ≈0.13±0.004).

The two methods to determine *g*-value have been developed and applied previously (Iwano and Danhara, 1998; Jonckheere and Van den haute, 2002; Jonckheere, 2003; Enkelmann and Jonckheere, 2003). In this work, these methods were applied to grains with random orientations and compared with the usual practice of measuring *g* on prismatic or basal extensive sections (Jonckheere, 2003).

As typically practiced, the EDM precludes the determination, for each apatite sample, of a mean induced confined fission-track length, which is used as proxy for the mean length of the unannealed confined spontaneous fission track and is normally referred to as initial confined fission-track length, L_0. Thus, L_0 is the reference to quantify the degree of annealing of a fission track, making it a key parameter for thermal history modeling.

In general, for modeling purposes, the fission-track researchers apply a standard L_0-value of 16.30μm, the mean of all values for Durango apatite reported by Green et al. (1986) and close to that reported by Carlson et al. (1999) or, if the sample is chemically characterized, adopt the value of L_0 for the sample with the closest chemical composition among those tabulated by Carlson et al. (1999) or Barbarand et al. (2003). Even if the sample composition matches exactly the one of a tabulated sample this procedure is risky.

The discussion above as well as discussions in Barbarand et al. (2003), Ketcham, (2005) and Ketcham et al. (2009), makes explicit the necessity of an adequate procedure for obtaining the thermal history modeling. The ideal situation is to obtain the L_0-value in the same laboratory and analysis criteria in which the spontaneous fission tracks were measured. Thus, a laborious but reliable alternative is to obtain the L_0-value directly in the apatite sample to be dated. This procedure can be done using the same pre-annealed aliquot, used to determine *g*-value described above, to measure the induced mean track lengths. Thus, the sample used to dating and thermal history modeling is also used for obtaining the L_0-value. Thus, even L_0 depending on the apatite chemical composition and lattice structure (Carlson et al. 1999; Barbarand et al. 2003), the direct measurement of this parameter for each sample makes thermal history modeling more accurate (Donelick et al. 2005; Ketcham et al. 2009).

To illustrate the proposed method, values of L_0 are measured in eight apatite samples from the crystalline rocks from Mantiqueira Mountain Range, Mar Mountain Range and adjacent areas of southeast, Brazil, (Tello et al. 2005). The influence of L_0-value in the thermal history modeling is then shown with a practical example. The same apatite sample has its thermal history modeled with values of L_0 in the range of values found in literature and in this work (14.9 to 16.7μm).

2. Method

2.1. Fission-track age equation

Fission-track ages can be calculated, by the ϕ-method, using the following equation (Jonckheere, 2003):

$$t = \frac{1}{\lambda_\alpha} \ln\left[1 + gL(\rho_S/\rho_i)(\lambda_\alpha/\lambda_F)(I\phi\sigma)\right] \quad (1)$$

In Eq. (1), λ_α is ^{238}U alpha decay constant; λ_F is the ^{238}U spontaneous fission decay constant; $\rho_s(\rho_i)$ is the spontaneous (induced) density; I is the isotopic concentration ratio, i.e., $\theta_{235}/\theta_{238}$; ϕ is the thermal neutron fluence; σ is the effective cross-section for fission of ^{235}U by thermal neutron capture; L is the ratio between induced and spontaneous fission tracks that indicate the degree of annealing experienced by the sample and g is the geometry factor (also referred to as *GQR*).

Several experimental procedures have been developed over the years for the calibration of the FT age equation, (Fleischer et al. 1975; Naeser et al. 1979; Greadow and Duddy, 1981; Hurford and Green, 1982; Storzer and Wagner, 1982). These procedures can be distinguished from each other mainly in the way the induced fission tracks are analyzed. The two most applied procedures are: Population Method, PM, and External Detector Method, EDM

The EDM allows for the individual grain dating. Thus, EDM can be applied, even for apatite belonging to sedimentary rocks. The IUGS (*International Union of Geological Sciences*) recommended that an absolute (ϕ-method) calibration with the accepted λ_F value could be used to date apatite together with PM analysis, whereas ζ-calibration is recommended in all fission-track techniques (including PM) (Hurford, 1990; Iwano and Danhara, 1998). This restriction is because in EDM the differences in efficiency between apatite and muscovite must be accounted for through the measurement of a geometry factor if the ϕ-method is applied (Naeser, 1967; Hurford, 1990; Iwano and Danhara, 1998).

Unlike PM, in which both spontaneous and induced tracks are measured under the same conditions, analyses with EDM are performed in minerals with different detection thresholds, chemical etching and observation and geometric efficiencies. In this way, the efficiencies do not cancel out and the geometry factor that ideally equals 0.5 has to be determined from separate experiments. The values found in literature can reach 0.61 (Enkelmann and Jonckheere, 2003).

2.2. Measurement of the geometry factor through projected fission-track length distributions

When EDM is applied, spontaneous fission-track densities are measured in apatite grains (under 4π geometry), whereas induced ones are measured in muscovite external-detector (under 2π geometry). Thus, the geometry correction is $G=(2\pi/4\pi)=1/2$. However, for EDM ages, both spontaneous and induced fission-track densities are measured in different detectors, so differences in the efficiency of revelation by etching and observation under microscopy should be considered. This parameter is the ηq value (Jonckheere and Van den haute, 1999).

The ηq-value in both an apatite internal surface and a muscovite external detector is determined by measuring induced fission tracks. For this, prior to irradiation, spontaneous fission tracks are totally annealed in the apatite sample. The apatite grains are mounted in epoxy resin polished and then attached to the muscovite external detector before irradiation. After irradiation, the assembly of apatite is polished again until the 4π geometry is attained, i.e., the layer removed is thicker than the fission-fragment range. Projected fission-track

This is a preprint, the final version is subject to change, of the American Mineralogist (MSA)
Cite as Authors (Year) Title. American Mineralogist, in press.
(DOI will not work until issue is live.) DOI: http://dx.doi.org/10.2138/am.2014.4140

lengths, which are the distances, parallel to the observation surface, between the etch pits and the ends of the tracks, are measured (Figure 1a).

According to Dakowski (1978) the number of tracks per unit volume, $N(z,\theta)$, can be written as:

$$N(z,\theta)dzd\theta = N\cos\theta dzd\theta \qquad (2)$$

The lower extremities of fission tracks are in the depth range from z to $z+dz$ and its inclination between θ and $\theta+d\theta$ (Jonckheere and Van den Haute, 1998) (Figure 1a). To obtain the frequency distribution $N(p,\theta)dpd\theta$, per unit volume of p and θ, a transformation of variables is necessary:

$$N(p,\theta)dpd\theta = N(z,\theta)\left|\frac{\partial z}{\partial p}\right|dpd\theta \qquad (3)$$

Combining and integrating these equations (Jonckheere and Van den haute 1998), yields the ideal projected length distribution for an internal mineral surface:

$$N(p)dp = N\left(1-\frac{p}{2l}\right)dp \qquad (4)$$

In Eq. (4), p is the projected length, which crosses the analyzed surface and l is the fully ($0\leq e\leq 2l$ for internal and $l\leq e\leq 2l$ for external surface) (figure 1a) etched length of the combined range of the fission fragments, which are propelled in opposite directions. The l-parameter is reported in Jonckheere and Van den Haute, (1999) as the R-parameter. This change was necessary because in this work the R-parameter is the range deficit factor value which makes part of GQR-value, following the convention given by Jonckheere, 2003 and defined below. In Figure 1b, examples of projected length distributions from apatite external surface obtained in this work are shown. Note that the shorter projected lengths are less abundant than expected by the ideal triangular distribution. For this method of

Always consult and cite the final, published document. See http://www.minsocam.org or GeoscienceWorld

determining ηq, it is assumed that all the loss in efficiency occurs for the shorter projected lengths. Longer tracks are then used to fit the theoretical distribution. The value of ηq is the ratio between the areas of the measured and ideal distributions. The same procedure is applied for internal and external surfaces of apatite and external-detector (Jonckheere and Van de Haute, 1998, 2002).

The etchable range of a track is not the same in apatite and in muscovite. A given track may be observed only in apatite or muscovite external-detector, in both or neither (Iwano et al. 1993; Jonckheere, 1995, 2003). Therefore, the introduction of a range deficit factor value (R) is required. The R-value is calculated by the relationship between latent (L_f -apatite, L'_f -muscovite) and etched (L_e-apatite, L'_e-muscovite) track lengths: $R=(L_f/L'_f)/(L'_e/L_e)$ (see discussion in Jonckheere, 2003). The geometry factor is, therefore, given by GQR, the product of $G(=2\pi/4\pi=1/2)$, $Q=[\eta q]_{ed}/[\eta q]_{is}$ and the range deficit factor value, R.

2.3. Measurement of the geometry factor through induced fission-track densities

Another way to obtain the geometry factor is the direct measurement of induced fission-track densities in both apatite internal surfaces and muscovite external-detector surfaces. The fission-track densities were determined counting all projected tracks which were measured to obtain the GQR value.

In this work, we propose an extension of this procedure, which consists of simultaneously dating unknown age samples by EDM and PM. The value of the geometry

This is a preprint, the final version is subject to change, of the American Mineralogist (MSA)
Cite as Authors (Year) Title. American Mineralogist, in press.
(DOI will not work until issue is live.) DOI: http://dx.doi.org/10.2138/am.2014.4140

factor is found by imposing that both dating protocols give the same ages. Rewriting the Eq. (1) for PM and EDM dating, respectively then yield:

$$t_{PM} = \frac{1}{\lambda} \ln\left[1 + g_{PM} L(\rho_S/\rho_i)(\lambda/\lambda_F)(I\phi\sigma)\right] \tag{5}$$

$$t_{EDM} = \frac{1}{\lambda} \ln\left[1 + g_{EDM} L(\rho_S/\rho_i)(\lambda/\lambda_F)(I\phi\sigma)\right] \tag{6}$$

In the Eq. (5) and (6), the *g*-parameters refer to population (PM) and external detector method (EDM), respectively. For simultaneously dating by EDM and PM, besides having to prepare the apatite/external detector mount, an aliquot or mount of pre-annealed apatite grains must be simultaneously irradiated with thermal neutrons. In this way, the constants (λ, λ_F and I), and irradiation parameters (□ and σ) are the same in Eqs. (5) and (6) and the ratio of these two equations results in:

$$\frac{\exp^{\lambda t_{PM}} - 1}{\exp^{\lambda t_{EDM}} - 1} = \frac{g_{PM}}{g_{EDM}} \left[\frac{L(\rho_S/\rho_i)_{PM} (\lambda/\lambda_F)(I\phi\sigma)}{L(\rho_S/\rho_i)_{EDM} (\lambda/\lambda_F)(I\phi\sigma)} \right] \tag{7}$$

Then, imposing the same fission-track age and degree of annealing (*L*-value), it follows from Eq. (7) that:

$$\frac{(\rho_S/\rho_i)_{PM}}{(\rho_S/\rho_i)_{EDM}} = \frac{g_{EDM}}{g_{PM}} \tag{8}$$

Considering uniformity in the uranium/surface track distribution, there is no reason why spontaneous densities should be different. Actually, the same apatite mount can be used to measure the spontaneous fission density in both dating protocols. Thus:

Always consult and cite the final, published document. See http://www.minsocam.org or GeoscienceWorld

$$\frac{(\rho_i)_{EDM}}{(\rho_i)_{PM}} = \frac{g_{EDM}}{g_{PM}} \tag{9}$$

Considering that for PM both spontaneous and induced fission-track densities are analyzed in apatite internal surface, the efficiency factor, g_{PM}, is assumed to be 1. Thus, the geometry factor for EDM dating can be determined as:

$$\frac{(\rho_i)_{EDM}}{(\rho_i)_{PM}} = g_{EDM} = g \tag{10}$$

The reason why the geometry factor (ideally $g_{2\pi}/g_{4\pi}$) assumes values different from ½ is that the ratio of efficiency factors does not cancel out, since etching and counting efficiencies are different in PM (induced tracks in apatite) and EDM (induced tracks in muscovite). For practical applications, the geometry factor must incorporate this effect. For direct comparison, geometry factor determined by measuring projected length distribution can be described in terms of $[GQR]_{\mathrm{is/ed}}$, where the parameter $G = (g_{2\pi}/g_{4\pi})$, $Q = [\eta q]_{\mathrm{ed}}/[\eta q]_{\mathrm{is}}$ and the range deficit factor value, R. Thus, $(\rho_i)_{EDM}/(\rho_i)_{PM}$ (that is by definition equal to ρ_{is}/ρ_{ed}) embraces the differences of etching and counting efficiencies between apatite and muscovite detectors which depend on Q and R parameters. In other words, the efficiency ratio is the product between $Q = [\eta q]_{\mathrm{ed}}/[\eta q]_{\mathrm{is}}$ and the range deficit factor value, R.

Eq. (10) is therefore, the same used when the g-value is determined through induced fission-track densities in both apatite internal surface and muscovite external detector. However, in this case, regular unknown age samples can be used to measure the g factor provided an extra aliquot or mount of apatite grains is irradiated along with the sample to be dated. Ideally, this procedure would make it possible to measure one individual g-value for each sample.

3. Experimental procedures

Durango apatite crystals were cut to expose extensive prismatic surfaces (Mn-1 and Mn-2), and two mounts composed of apatite grains at random orientations (D-2 and D-3), were assembled for this experiment. Samples from crystalline basement (TF-5, TF-9, TF-10, TF-12, TF-17, TF-21, TF-30, TF-32 and TF-42), collected in the State of São Paulo, Brazil (Tello et al. 2005), were also used. Samples used to obtain the geometry factor were heated at 450°C for 24 hours. This heating is sufficient to erase the spontaneous fission tracks (total annealing). Samples were ground and polished, attached to muscovite (external detector) and irradiated with thermal neutrons to induce ^{235}U fission. Neutron fluence was ≈3.0×10^{15}neutrons/cm^{-2}. The ^{235}U induced-fission fragments that escape the mineral through the surface can be detected by the external detector, forming a mirror image of the grain contained in the mount. To obtain an internal surface, the irradiated apatite samples were ground and polished again. This was necessary because the surface attached to muscovite collected tracks only from below (2π geometry). The surface obtained after irradiation and polishing collected tracks from below and from above (4π geometry). The polishing after irradiation to reach an internal surface removed a layer just a little thicker than the range of a fission fragment. All etched fission-tracks in an external surface were totally erased. The removed layer is very thin compared with the dimensions of the grains we usually analyze and there is almost no change in surface area. These samples were used for the measurement of the geometry factor through the ratio between densities, ρ_{ed}/ρ_{is}, and *GQR* measurement through projected length distribution.

Always consult and cite the final, published document. See http://www.minsocam.org or GeoscienceWorld

Samples from crystalline rocks were divided in three aliquots: two for PM and one for EDM dating. For PM, an aliquot was used for the determination of the spontaneous-track density and the other was pre-annealed in the same way as described above and irradiated with thermal neutrons to induce ^{235}U fission. Once spontaneous and induced track densities are determined, both in apatite, PM fission-track ages were calculated.

For EDM, samples were mounted, spontaneous fission tracks were revealed by etching, and the mounts were attached to muscovite plates (external detector) for thermal neutron irradiation. Once spontaneous and induced densities in apatite and muscovite external-detector, respectively, are determined, EDM fission-track ages are calculated as functions of the geometry factor. Combining the induced densities obtained in both dating procedures, the geometry factor was using Equation (10).

Samples were irradiated at the IEA-R1 reactor (IPEN/CNEN, São Paulo, Brazil) using standard glasses (CN5), calibrated through natural uranium thin films, as dosimeters (Bigazzi et al. 2000; Iunes et al. 2002, 2004, 2005). The neutron fluence was measured using the calibration by natural uranium thin film yielding the value of ϕ=2,2×10^{15}neutrons/cm^2. One irradiation was done using a wrapper of cadmium and no significant fission track content was observed, indicating that no significant influence of epithermal/fast neutrons was present.

All apatite samples analyzed in this work were mounted in epoxy resin and had the same sanding (with sandpaper of #1200, 2400 and 4000), polishing (with diamond paste of 1 and ¼ µm) and etching. For apatite, the etching was carried out in a 5% NHO_3 solution, at 20 ºC, for 55 seconds (Tello et al. 2003, 2005, 2006). Muscovites were etched in a 48%

HF solution, at 15 ºC, for 90 minutes. All etching procedures were carried out in an ultrathermostatic bath SP Labour model SP-152/30. Variation in temperature was ≈0.1°C.

Density and projected length measurements were carried out using a Zeiss Axioplan 2 Imaging microscope, with nominal magnification of 1000×, dry. In order to identify the orientation of each grain, the etch figures and other surface etching figures were taken into account. Random orientation means that grain surfaces with any orientation but basal section (or close to) were not used. Basal section shows the etch figure (etch-pyramid geometry), which can be easily distinguished. Prismatic section usually appears to be a clear surface with etch pits (D_{par}) parallel the crystallographic C-axis. Other orientations are those, in which crystal surface was not clear (e.g., textured surface) or when the etch pit is not well oriented. (Jonckheere and Van den Haute, 1996). For the samples employed in this work approximately 40% of the grains were prismatic, 15% were basal or close to (not analyzed) and 45% were at other orientations.

4. Results and Discussion

4.1. Geometry factor

Geometry factor data using projected length distributions were measured and the values of ηq and *GQR* were determined (Table 1). The errors for ηq measurements are the averages, which consider the combination between minimum and maximum interval considered for a triangular fit. For density measurements, the relative errors are Poissonian, i.e., $(1/\sqrt{N})$, where N is the number of counted tracks.

The average of $[GQR]_{\mathrm{ed/is}}$ values (last column) for samples containing grains at random orientation, D-2 and D-3, is 0.59±0.01. For extensive surface samples, Mn-1 and Mn-2, the average is 0.60±0.01. These values are internally consistent and compatible with the data presented in Jonckheere (2003). For crystalline basement sample, TF-42, the geometry factor value is 0.56±0.03. Considering the greater error for sample TF-42, $[GQR]_{\mathrm{ed/is}}$ values are also compatible.

For these same samples, density measurements are also shown in Table 1. The values of g obtained by the ratio ρ_{ed}/ρ_{is} are shown in the sixth column. The average value for g between random-oriented grain samples D-2 and D-3 is 0.58±0.01. This value does not differ from data determined in this work by measuring $[GQR]_{\mathrm{ed/is}}$ and presented in Jonckheere (2003). For extensive surface samples, Mn-1 and Mn-2, the average is 0.55±0.02, which is, in two deviations, close to the 0.60±0.01. But, as the values are not contained in the error bars, we cannot be conclusive about the compatibility of these values. For crystalline basement sample, TF-42, the value is 0.53±0.02, in agreement with value determined by $[GQR]_{\mathrm{ed/is}}$ using the same sample and the average of Mn-1 and Mn-2. Measurements in Durango apatite samples are statistically in agreement.

Geometry factor values obtained through ρ_{ed}/ρ_{is} are systematically lower than $[GQR]_{\mathrm{ed/is}}$ values, which may be an artifact of considering the projected length distribution as generated by tracks with only one average length, which results in the triangular distribution of Eq. (4). In fact, the two fragments propelled in the fission process have different masses and ranges and, therefore there should be two mean track lengths. Guedes et al. (2008), studying tracks from uranium and thorium thin films detected in muscovite, were able to distinguish the distributions of projected track lengths of lighter and heavier fragments. In thick source geometry, this distinction is not so clear, but has a visible effect at the longer length end of the distribution.

Note that, for the two methods, the values of *g* found for TF-42 are lower than the values found for the Durango apatite mounts. However, although this difference is larger for $[GQR]_{\mathrm{ed/is}}$ values, error bars do not allow the conclusion that efficiency has changed. For this reason, it is appropriate to analyze the geometry factors obtained for other basement rock samples.

Geometry factors calculated for eight basement samples, according to Eq. (10), are shown in Table 2. The reduced chi-square for sample TF-17 shows that more than one grain population may be mixed in this sample, which is possible even for basement rock samples (e.g., O'Sullivan and Parrish, 1995). This sample has the most divergent *g* value. To test its influence in the dataset, the χ^2 test was applied to the entire set including TF-17 and then without this sample. The weighted average of these geometry factors for the former case is 0.56±0.02 ($\chi^2_\nu \approx 1.34$; $P_\nu(\chi^2_\nu) \approx 0.23$). For the latter case, the weighted average of these geometry factors also is 0.56±0.02 ($\chi^2_\nu \approx 1.08$; $P_\nu(\chi^2_\nu) \approx 0.38$). These values are internally consistent and the reduced chi-square suggests that geometry factors could be drawn from the same population. Perhaps, the scatter in data appears because the data are based on a relative small track/count, an intrinsic characteristic of these samples. Comparing this value with the average values for the prismatic sections of Durango (Mn-1 and Mn-2) and for the Durango samples containing grains at random orientation (D-2 and D-3), no statistically significant difference is observed. While this should not be taken as general rule, the counting efficiency did not show an important difference between analyzing grains at prismatic or random orientation.

As stated before, the method presented in this work allows the measurement of a value of *g* for each dated sample. For instance, the ages of the eight basement samples used to determine *g* were calculated using Eq. (1). Ages presented are EDM, which, using the geometry factors shown in Table 2, are (by definition) identical to PM ages (e.g. Grimmer et al. 2002; De Grave and Van den haute, 2002). The last column of Table 2 shows the results for the χ^2 test for the individual grain ages of each sample. The probability density, *P*, present acceptable values (in most case are around 100%) showing that it is safe to apply the PM protocol to these samples.

Fission-track ages were calculated using the $[GQR]_{\mathrm{ed/is}}$ values determined with Durango apatite and TF-42. The ages were also calculated using the ρ_{ed}/ρ_{is} ratio values determined with TF-42 and with the average presented in Table 2 and plotted against those calculated with individual *g*-value (Figure 2) (in the last case, the values were plotted together considering that they give the same results. The larger error between these samples was used in the plot). Although the magnitude of the errors do not allow further discussions, it is possible to verify that the choice of the g-value has an influence on the age calculation as it can be seen in the plots of residuals (Figure 2d,e,f). A better fit in ages occur when geometry factors are determined with apatite from basement rock rather than Durango one. Using the presented method, it is possible to build a database of geometry factor values for different apatite species, just as Donelick et al. (2005) have suggested for the length of the unannealed fission tracks (discussion below). This database would allow for using a, at least closely, adequate geometry factor, even in situations, in which it is not possible to measure a value of *g* for each sample, i.e., when the number of apatite grains is not sufficient to an additional mount to be irradiated together with the EDM mount. This database can be built with samples that present enough apatite grains so that the count can give an acceptable error. As an example, if we consider the sample whose error in age is around 5%, then measuring approximately 625 induced tracks in apatite (Poissonian error around 4%) the final errors is around 6.4%, a value still acceptable for fission-track dating. For larger error in age, the geometry factor error described above becomes less significant. It is important to consider that the number of tracks in this case, depends also on uranium content in the samples as well as on the neutron irradiation. Furthermore, with automatized measurements (Gleadow et al. 2009) this procedure becomes less arduous and can result in smaller statistic deviations.

Note also that the values of *g* presented in this work are in the range of values presented in literature: 0.51±0.02 (Gleadow and Lovering, 1977); 0.55±0.02 (Iwano and Danhara, 1998); 0.61±0.01 (Enkelmann and Jonckheere, 2003).

4.2. Horizontal confined induced fission tracks

The lengths of the horizontal confined induced fission tracks have been measured. The values found for these samples can vary up to ≈6%, from 14.9 to 16.0μm and values up to 16.7μm can be found in literature (Carlson et al. 1999). As indicated in the introduction, an advantage of irradiating pre-annealed apatite samples together with the EDM assembly is the possibility of measuring the initial fission-track length (lengths of the unannealed fission-tracks), L_0, which is a necessary input for modeling thermal histories and is a natural

Always consult and cite the final, published document. See http://www.minsocam.org or GeoscienceWorld

output in PM dating (Tello et al. 2003, 2005, 2006; Ribeiro et al. 2005). It turns out that as EDM is currently the most applied dating method, the practice of measuring L_0 was abandoned because, for EDM, induced tracks are registered in muscovite. For modeling, literature values are often adopted, which may yield inaccurate thermal histories, since values of L_0 may vary significantly from one sample to another (Table 2) and among analysts (Ketcham et al. 2009). Donelick et al. (2005) suggested a database composed of unannealed lengths of apatite samples. They suggest that 50 or more apatite species with different chemical compositions would give significant additional information.

The method suggested in this paper would allow the measurement of a L_0 for each apatite and, at the same time, contribute to the formation of a database to be used in cases in which the measurement of L_0 is not possible. One such example of this is the determination of the fission-track age via LA-ICP-MS. In this case, uranium content is determined via mass spectrometry and neutron irradiation is not necessary (Hasebe et al. 2004; Hadler et al. 2009, Ito and Hasebe, 2011).

To illustrate the impact of L_0 in thermal history modeling, one of the samples analyzed for measurements of g and L_0, TF-10, was modeled with different values of the initial fission track length. This sample belongs to Mantiqueira mountain range, Southwest Brazil. It has been shown (Tello et al. 2003, 2005; Gallagher and Brown, 1999) that the geological evolution of Mantiqueira is related to South Atlantic Ocean opening (e.g., Larson and Ladd, 1973).

This sample was chosen because of the good number of both spontaneous and induced horizontal confined fission tracks that could be measured, respectively 185 and 129 (Figure 3). However, it can be seen in Table 2 that other samples have a smaller number of induced horizontal confined fission tracks. To illustrate how robust the results are, the sample TF-10 was also used. The test consists in calculating the average of induced horizontal confined fission tracks for subsets of randomly chosen lengths, taken from the entire set of lengths measure for TF-10. Thus, the averages were calculated for 129 (Table 2), 100, 70, 40 and finally 20 confined fission-tracks. The results are: 15.80±0.14, 15.82±0.16, 15.84±0.19, 15.83±0.26 and 15.67±0.42, respectively. All results are in agreement within 1σ. The difference concentrates mainly in the error, being larger when the numbers of confined fission-tracks become lesser. This result indicates that mean track lengths can be accurately (although less precisely) found even when only about 20 tracks have their lengths measured.

Thermal histories were modeled with the computer program HeFTy (version 1.7.5) (Ketcham, 2005). The fanning curvilinear annealing equation (Ketcham et al. 2007) was assigned. Two comprehensive Monte Carlo boxes were initially chosen, in order to search for general trends in thermal history model. Firstly, for the segment parameter, values of zero for "Halve segments" and "Episodic" for "Randomizer style" were used. In this way, only segments with their end points inside Monte Carlo boxes are randomly chosen and any subdivision of the thermal histories between constraint boxes was forbidden, maximizing the simplicity of the thermal histories tested. The merit value for accepted fit was the conventional 0.05. We chose the values of L_0 to vary in the range of values obtained in this work and presented in the literature (Carlson et al. 1999), 14.9 to 16.7μm. The thermal histories modeled with the different values of L_0 are shown in Figure 4. The most pronounced variation is in the final cooling episode, which becomes faster as the value of L_0 increases. This trend is more clearly observed in Figure 5, which shows the relationship between cooling rate and the L_0 value. Note in Figure 4 that time-temperature (t-T) paths for shorter of L_0-values, enter the partial-annealing zone (PAZ) earlier. The slope of the t-T path is more quickly inverted towards the present day temperature, in such a way that their PAZ residence time is shorter and more tracks are generated in the final part (closer to time zero), at lower temperatures, and are thus less annealed. As, for longer values L_0-values, the t-T path exit of the partial annealing zone starts later, a faster cooling until present temperature is predicted.

The thermal histories were also modeled with one segment parameter and keeping the Episodic for Randomizer style and the results were similar.

Finally, using the latter configuration, thermal histories were modeled, but this time, the midpoint of the first constraint box was placed at slightly higher-temperature than the second one. As it is possible to see in Figure 6, the thermal histories in this case are monotonic cooling. This indicates that the choice of constraints is crucial and has a big effect on the models. It is again observed that the residence inside the partial annealing zone is longer for greater values of L_0.

Finally, the thermal histories of the Figure 6(c) show that the samples entered in partial annealing zone ≈130Ma, the age of the ocean opening. This indicates that the latter constraints chosen for the thermal history modeling presented here yield more compatible geological predictions than the first one.

4.3. Implications for the ζ-calibration

All values for the geometry factor presented above are independent from the neutron dosimetry, as they result either from projected length measurements or from ratios of induced densities in mounts of the same apatite samples, irradiated together. In this way, the values of g and L_0 could also have been determined by practitioners of the zeta method. The g factor appears in the ζ-age equation (for instance, Donelick et al. 2005):

$$t = \frac{1}{\lambda}\ln\left[1 + \lambda\zeta g\rho_d \frac{\rho_S}{\rho_I}\right] \tag{11}$$

In Eq. (11), ρ_d is the induced fission-track density for a uranium dosimeter glass used to monitor neutron fluence during neutron irradiation, ζ is the calibration factor, which depends on the analyst efficiency, on the dosimeter glass and on the age of an apatite standard, usually Durango. The other symbols are the same as for Eq. (1). The ζ-calibration factor is found inverting Eq. (11) for the standard sample:

$$\zeta = \frac{\exp(\lambda t_{STD} - 1)}{g_{STD}\lambda\rho_d\left(\rho_S / \rho_I\right)} \tag{12}$$

where the sub-index *STD* refers to the standard sample. Note that the geometry factor appears also inside ζ. It is normally assumed that the geometry factor is the same in both standard and unknown age sample. However, unknown samples normally present inclusions or defects visible after etching and thus may not present exactly the same efficiency compared with high-quality Durango apatite. Nevertheless, the g-value implicit in the calculation of the zeta parameter (measured with Durango apatite) may not be the same g-value that represents the unknown samples. Thus, a more accurate approach would be to determine g_{STD}, instead of assuming g_{STD}=0.5, and the value of g for that sample. In this way, the eventual differences in efficiency are accounted for.

4.4. Projected length distribution for TF through LA-ICP-MS

Always consult and cite the final, published document. See http://www.minsocam.org or GeoscienceWorld

As presented above, the determination of $[\eta q]_{is}$ through projected length for spontaneous fission-track measurements is important for LA-ICP-MS FT ages. For direct dating, assuming that the uranium content is accurately determined, the efficiency parameter to find is $[\eta q]_{is}$, which appears in the direct dating age equation:

$$t = \frac{1}{\lambda_\alpha} \ln\left[1 + \frac{\lambda_\alpha}{\lambda_F} \frac{1}{g_{4\pi}[\eta q]_{is} r_S} \frac{\rho_S}{N_{238}}\right] \tag{13}$$

In equation (13) r_s is the mean length of horizontal spontaneous fission tracks and N_{238} is the number of uranium atom per volume unit which can be calculated through equation presented in Hasebe et al (2004).

The $[\eta q]_{is}$ is calculated by comparing theoretical and experimental distributions of projected track lengths which allows one to quantify the efficiency of etching and observation. On the other hand, when LA-ICP-MS is applied, the determination of L_0-value assumes the same importance described for EDM. This means that a database containing the most comprehensive set of apatite species should be built with information and measurements similar to those presented in Barbarand et al. (2003).

5. Conclusion

New values for geometry factors, obtained through projected length distributions and the ratio between induced fission-track densities in muscovite external detector and apatite, were presented. For this, five apatite samples have been used, two of which were extensive surface (Mn-1 and Mn-2, Durango apatite) in prismatic section and three random

Always consult and cite the final, published document. See http://www.minsocam.org or GeoscienceWorld

This is a preprint, the final version is subject to change, of the American Mineralogist (MSA)
Cite as Authors (Year) Title. American Mineralogist, in press.
(DOI will not work until issue is live.) DOI: http://dx.doi.org/10.2138/am.2014.4140 1/16

orientation grain mounts (D-2 and D-3, Durango apatite and TF-42, from crystalline rock). No significant differences were observed among the obtained values.

The average value of the geometry factors found for basement samples (measured in random orientation grains) is statistically in agreement with the values measured for Durango samples, both in prismatic sections and random orientation grain samples. This result indicates the possibility of dating non prismatic section grains in cases in which there is a paucity of grains, as is the case, for instance, for many basin samples.

With an example, it was illustrated how the value of L_0 determines the modeled residence of the sample inside the partial annealing zone, showing the important role of the L_0-value for thermal history modeling. In this way, the possibility of measuring this parameter in the same sample and at the same analysis conditions at which the spontaneous tracks are measured, including etching, microscopy equipment and analyst observation criteria, should be considered. An extension of the usual method of measuring *g*-value was also shown that makes it possible to obtain an individual value of L_0 for each sample to be dated.

The possibility of obtaining *g*-values when the ζ-calibration is applied is advisable because the geometry factor measured for the standard may be different from the geometry factor measured for the unknown age sample.

The procedures we propose in this work make FTT more laborious because more analysis work is necessary, but also because more grains are needed for the additional mount. Ideally, approximately the same number of grains needed for spontaneous track counting would be needed for the additional mount. However, considering that the irradiation may be controlled for generating as many induced tracks as necessary, the

Always consult and cite the final, published document. See http://www.minsocam.org or GeoscienceWorld

(DOI will not work until issue is live.) DOI: http://dx.doi.org/10.2138/am.2014.4140

number of additional grains will be constrained by grain availability in sample. In spite of the extra work, the proposed procedures contribute to increase the accuracy of data analysis, mainly for thermal history modeling. For dating, these procedures for determination of g are justifiable in cases where the observation efficiency is considerably different between the sample used to obtain g-value (e.g. standard Durango apatite) and the unknown age sample. For example, basin samples contain commonly different apatite populations that might merit a more rigorous investigation of their etching, annealing and geometry properties.

In addition, if LA-ICP-MS is used for FT dating, the g-value may not be used anymore, but, the $[\eta q]_{is}$ for spontaneous fission tracks becomes an important parameter to be determined.

ACKNOWLEDGEMENTS

We thank Richard Ketcham and Jocelyn Barbarand for their constructive comments that helped improve the manuscript. This work is part of Soares's PhD research and was financially supported by Fundação de Amparo à Pesquisa do Estado de São Paulo (FAPESP, Brazil) and Conselho Nacional de Desenvolvimento Científico e Tecnológico (CNPq, Brazil).

Always consult and cite the final, published document. See http://www.minsocam.org or GeoscienceWorld

Reference

Barbarand, J.,Carter, A., Hurford, T., Wood, I. (2003) Compositional and structural control of fission-track annealing in apatite.Chemical Geology, 198, 107-137.

Bigazzi, G., Guedes, S., Hadler N., J.C., Iunes, P. J., Paulo, S.R. and Tello S., C.A. (2000) Application of neutron dosimetry by natural uranium and thorium thin films in Fission Track Dating. In: 9th International Conference on Fission Track Dating and Thermocronology, Book of Extend abstracts Lorne, Australia, 33-35.

Carlson, W.D., Donelick, R.A., Ketcham, R.A. (1999) Variability of apatite fission-track annealing kinetics: I. Experimental results. American Mineralogist, 84, 1213-1223.

Dakowski, M (1978) Length distribution of fission tracks in thick crystal. Nuclear Track Detection, 2, 181-189.

De Grave, J., Van den haute, P. (2002) Denudation and cooling of the Lake Teletskoye region in the Altai Mountains (South Siberia) as revealed by apatite fission-track thermochronology. Tectonophysics, 349, 145-159.

Donelick, R.A., O Sullivan, P.B., Ketcham, R.A. (2005) Apatite fission-track analysis. Rev. Mineralogy Geochemistry, 58, 49-94.

Enkelmann, E., Jonckheere, R. (2003) Correction factors for systematic errors related to the track counts in fission-track dating with external detector method. Radiation Measurements, 36, 351-356.

Fleischer, R.L., Price, P.B., Walker, R.M. (1975) Nuclear tracks in solids: Principles and Applications. University of California Press, Berkeley.

Franco-Magalhães, A.O.B., Hackspacher, P.C., Glasmacher, U.A., Saad, A.R. (2010) Rift to post-rift evolution of a passive cpntinental margin: The ponta Grossa Arch, SE, Brazil. International Journal of Earth Science, 99, 1599-1613.

Gleadow, A.J.W., Duddy, I.R. (1981) A natural long-term track annealing experiment for apatite. Nuclear Tracks, 5, 169-174.

Gallagher, K., Brown, R. (1999) The Mesozoic denudation of the Atlantic margins of southern Africa and southeast Brazil and the relationship to offshore sedimentation. In: CAMERON, N.R.; BATE, R.H.; CLURE, V.S. (Eds.). The Oil and Gas Habitats of the South Atlantic. Geol. Soc. London, Special Publications. 153, 41-53.

Gleadow, A.W. and Lovering, J.F. (1977) Geometry factor for external detector in fission track dating. Nuclear Tracks, 4, 91-100.

Always consult and cite the final, published document. See http://www.minsocam.org or GeoscienceWorld

Gleadow A.J.W., Belton D.X., Kohn B.P., Brown R.W. (2002) Fission track dating of phosphate minerals and the thermochronology of apatite. Review in Mineralogy and Geochemistry, 48, 579-630.

Gleadow, A.J.W., Gleadow, S.J., Belton, D.X., Kohn, B.P., Krochmal, M.S. (2009) Coincidence Mapping: a key strategy for automated counting in fission-track dating. In: Ventura, B., Lisker, F. and Glasmacher, U.A. (eds.), Thermochronological methods: from paleotemperature constraints to landscape evolution models. Geological Society of London Special Publication, 324, 25-36.

Green P.F., and Durrani, S.A. (1978) A quantitative assessment of geometry factor for use in fission track study. Nuclear Tracks Detection, 2, 207-213.

Green, P.F., Duddy, I.R., Gleadow, A.J.W., Tingate, P.R., Laslett, G.M. (1986) Thermal annealing of fission tracks in apatite 3: a qualitative description. *Chem Geol. Isot Geosci Sect.* **59,** 237-253.

Grimmer, J.C., Jonckheere, R., Enkelmann, E., Ratschbacher, L., Hacker, B.R., Blythe, A.E., Wagner, G.A., Wu, Q., Liu, S., Dong, S. (2002) Cretaceous−Cenozoic history of the southern Tan-Lu fault zone: apatite fission-track and structural constraints from the Dabie Shan (eastern China). Tectonophysics, 197, 87-110.

Guedes, S., Jonckeere, R., Iunes, P.J., Hadler, J.C. (2008) Projected-length distributions of fission-fragment tracks from U and Th thin film sources in muscovite. Nuclear Instruments and Methods in Physics Research B, 266, 786-790.

Hadler, J.C., Iunes, P.J., Tello, C.A., Chemale, F., Kawashita, K., Curvo, E.A.C., Santos, F.G.S., Gasparini, T.E., Moreira, P.A.F.P., Guedes, S. (2009) Experimental study of a methodology for Fission-Track Dating without neutron irradiation. Radiation Measurements, 44, 955-957.

Hasebe, N., Barbarand, J., Jarvis, K., Carter, A., Hurford, A. (2004) Apatite fission-track chronometry using laser ablation ICP-MS. Chemical Geology, 207, 135-145.

Hurford, A.J. (1990) Standardization of fission track dating calibration. Recommendation by the Fission Track Workshop Group of the I.U.G.S. Subcommission on Geochronology, Chemical Geology, 80, 171-178.

Hurford, A.J., Green, P. F. (1982) A user's guide to fission track dating calibration. Earth and Planetary Science Letters, 59, 343-354.

Ito, K., Hasebe, N. (2011) Fission-track dating of Quaternary volcanic glass by stepwise etching. Radiation Measurements, 46, 176-182.

Iunes, P.J., Hadler, J. C., Bigazzi, G., Tello, C.A., Guedes, S., Paulo, S.R. (2002) Durango apatite fission-track dating using length-based age corrections and neutron fluence measurements by thorium thin films and natural U-doped glasses calibrated through natural uranium thin films. Chemical Geology, 187, 201-211.

Iunes, P.J., Hadler, J.C., Bigazzi, G., Guedes, S., Zuñiga, A., Paulo, S.R., Tello, C.A., 2004. Uranium and thorium film calibrations by particle track techniques. Journal of Radioanalitical and Nuclear Chemistry, 262, 461-468.

Iunes P.J., Bigazzi, G., Hadler, J.C., Laurenzi, M.A., Balestrieri, M.L., Norelli, P., Osório, A.M., Guedes, S., Tello, C.A., Paulo, S.R. (2005) U and Th thin film neutron dosimetry for fission-track dating: application to the age standard Moldavite. Radiation Measurements, 39, 665-668.

Iwano, H., Danhara, T. (1998) A re-investigation of the geometry factor for fission-track dating of apatite, sphene and zircon. In: Van den Haute, P.; De Corte, F. (Eds.), Advances in fission Track Geochronology, vol 10, Kewwer Academic Publishers, Dorcrecht: 47-66.

Iwano, H., Kasuya, M., Danhara, T., Yamashita, T., Tagami, T. (1993) Track counting efficiency and unetchable track range in apatite, Nuclear Tracks and Radiation Measurements, 21, 513-517.

Jonckheere, R. (1995) Absolute age determination of apatite based on uranium fission tracks: a methodical investigation. 504 p. Ph.D. Thesis. University of Gent, Belgium, (in Flemish).

Jonckheere, R. (2003) On the densities of etchable fission track in a mineral and co-irradiated external detector with reference to fission-track dating of minerals. Chemical Geology, 200, 41-58.

Jonckheere, R., Van den haute, P. (1996) Observations on the geometry of etched fission tracks in apatite: implications for models of track revelation. American Mineralogist, 81, 1476–1493.

Jonckheere, R., Van den haute, P. (1998) On the frequency distribution per unit area of the dimension of fission track revealed in an internal and external mineral surface and in the surface of an external detector. Radiation Measurements, 29, 135-143.

Jonckheere, R., Van den haute, P. (1999) On the frequency distribution per unit area of the projected and etchable length of surface-intersecting fission tracks: influences of track revelation, observation and measurement. Radiation Measurements, 30, 155-179.

Jonckheere, R., Van den haute, P. (2002) On the efficiency of fission-track counts in an internal and external apatite surface and in a muscovite external detector, Radiation Measurements, 35, 29-40.

Ketcham, R.A. (2005) Forward and inverse modeling of low-temperature thermochronometry data. Review of Mineralogy Geochemistry, 58, 275–314.

Ketcham, R.A., Carter, A.C., Donelick, R.A., Barbarand, J., Hurford, A.J. (2007) Improved modeling of fission-track annealing in apatite. *Am. Mineral.* **92,** 799-810.

Ketcham, R.A., Donelick, R., Balestrieri, M.L., Zattin, M. (2009) Reproducibility of apatite fission-track length data and thermal history reconstruction. Earth and Planetary Science Letters, 284, 504-515.

Larson, R.L., and Ladd, J.W. (1973) Evidence for Opening of the South Atlantic in the Early Cretaceous. *Nature.* **246,** 209, 212.

Naeser, C.W. (1967) The use of apatite and sphene for fission track age determination. Geological Society of America Bulletin, 78, 1523-1526.

Naeser, C.W., Gleadow, A. J. W., Wagner, G. A. (1979) Standardization of fission-track data reports. Nuclear Tracks, 3, 133-136.

O'Sullivan P.B. and Parrish R.R. (1995) The importance of apatite composition and single-grain ages when interpreting fission track data from plutonic rocks: a case study from the Coast Ranges, British Columbia. Earth and Planetary Science Letters. 132:213-24.

Ribeiro, L.F.B., Hachspacher, P.C., Ribeiro, M.C.S., Hadler, J.C., Tello, C.A., Iunes, P.J., Franco-Magalhães, A.O.B. (2005) Thermotectonic and fault dynamic analysis of precambrian basement and tectonic constraints within the Paraná Basin, Radiation Measurements, 39, 669-675.

Soares, C.J., Guedes, S., Curvo, E.A.C., Hadler, J.C., Jonckheere, R., Tello, P.T.D., Siqueira. T.T.D., Madi Filho, T. (submitted) Recalibration of dosimeter glasses through natural uranium thin film. Contributions to Mineralogy and Petrology.

Storzer, D., Wagner, G. A. (1982) The application of fission track dating in stratigraphy: a critical review. In G. S. Odin (ed.), "Numerical Dating in Stratigraphy", Wiley, Chichester, 199-221.

Tello, C.A., Hackspacher, P., Hadler, J.C., Iunes, P.J., Guedes, S., Paulo, S.R., Ribeiro, L.F. (2003) Recognition of Cretaceus, Paleocene and Neogene Tectonic Reactivation, through Apatite Fission-Track Analysis, in Precambrian areas of the Southeast Brazil: Association with the South Atlantic Ocean Opening. Journal of South American Earth Science, 15, 765-774.

Tello, C. A., Hadler, J.C., Iunes, P.J., Guedes, S., Hackspacher, P.C., Ribeiro, L.F., Paulo, S.R., Osório A.M. (2005) Thermochronology of the South American platform in the State of São Paulo, through apatite fission tracks. Radiation Measurements, 39, 635-640.

Tello, C. A., Palissari, R., Hadler, J.C., Iunes, P.J., Guedes, S., Curvo., E.A.C., Paulo, S.R. (2006) Annealing experiments on induced fission tracks in apatite: Measurements of horizontal-confined track lengths and track densities in basal sections and randomly oriented grains. American Mineralogist, 91, 252-260.

Figure Captions

Figure 1. (a) Schematic picture of measurements of projected length, (b) theoretical (full line) and experimental (dashed lines) for projected length distribution. The theoretical distribution represents the case of no track loss. In the experiment, every track usually counted for density measurements has its projected length measured. Short track lengths are under-represented compared to the expected distribution for the ideal case of perfect efficiency.

Figure 2. Age distribution applying different geometric factor values. (a) $[GQR]_{\mathrm{ed/is}}$ (Durango), (b) ρ_{es}/ρ_{is} (TF-42) and (c) $[GQR]_{\mathrm{ed/is}}$ (TF-42) and average of individual *g*-values. Also, the plots of residuals for (d) $[GQR]_{\mathrm{ed/is}}$ (Durango), (e) ρ_{es}/ρ_{is} (TF-42) and (f) $[GQR]_{\mathrm{ed/is}}$ (TF-42)

Figure 3. (a) Spontaneous and (b) induced horizontal confined fission tracks (sample TF-10).

Figure 4. Thermal histories for different values of L_0, as modeled using HeFTy. The dark blue line is the weighted mean of all fitted histories. Path segments between constraints (boxes) were not subdivided (i.e. "Halve Segments" input parameter set to 0), and the "Episodic" randomizer style was used.

Figure 5. Relationship between cooling rate during final cooling episode of each thermal history inversion in Fig. 4 and the L_0-value.

Figure 6. Thermal histories for different values of *L0*, as modeled using HeFTy, with constraint boxes (compared to Fig. 4) shifted so that histories are forced to have monotonic cooling. Parameter otherwise same as in Figure 4, except path segments between constraints are subdivided once (i.e. "Halve Segments" parameter set to 1).

(DOI will not work until issue is live.) DOI: http://dx.doi.org/10.2138/am.2014.4140

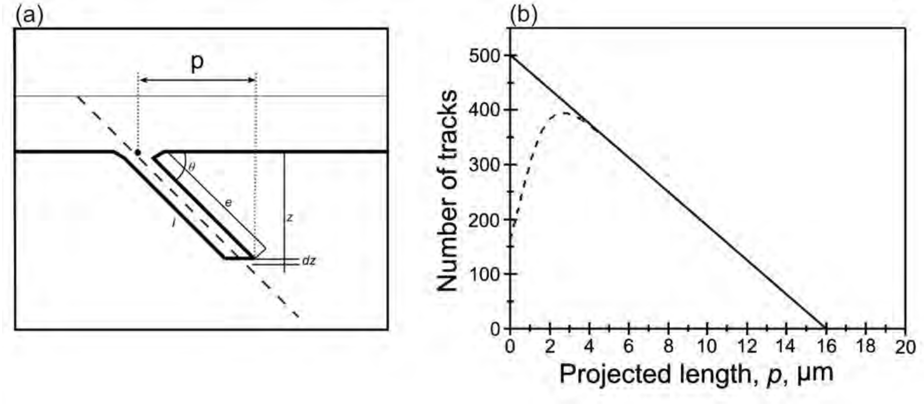

Always consult and cite the final, published document. See http://www.minsocam.org or GeoscienceWorld

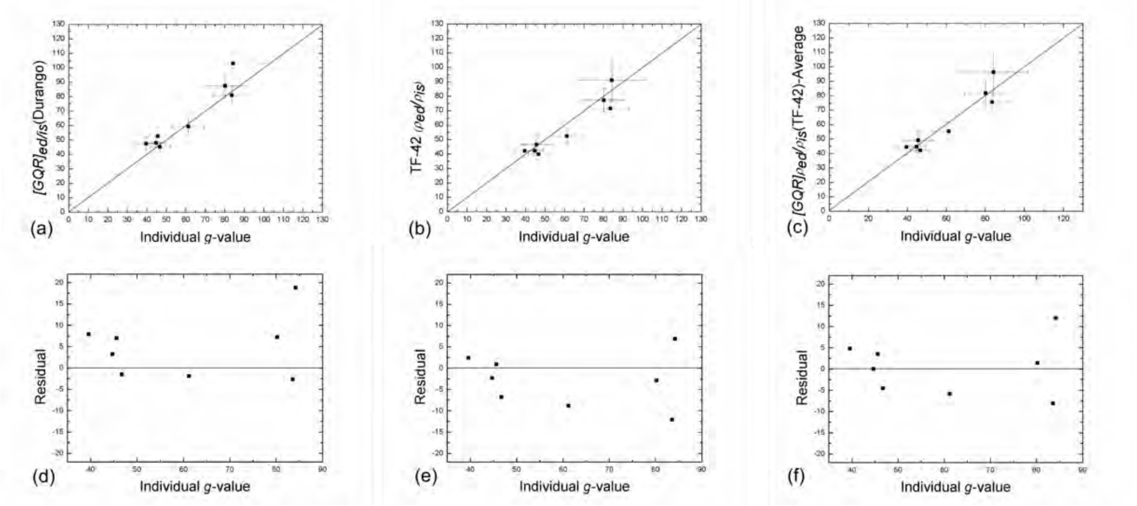
[GQR]ed/is(Durango)
TF-42 (ρed/ρis)
[GQR]ρed/ρis(TF-42)-Average
Residual
Individual g-value
(a)
(b)
(c)
(d)
(e)
(f)

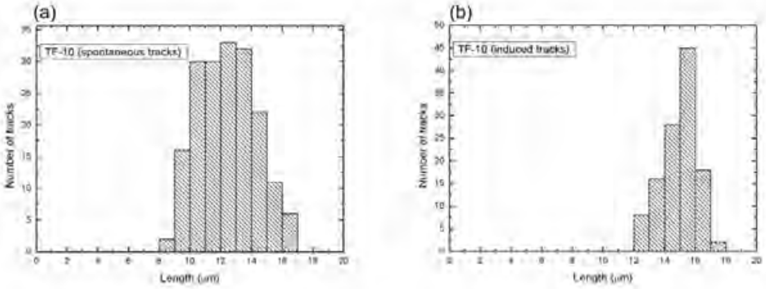

Always consult and cite the final, published document. See http://www.minsocam.org or GeoscienceWorld

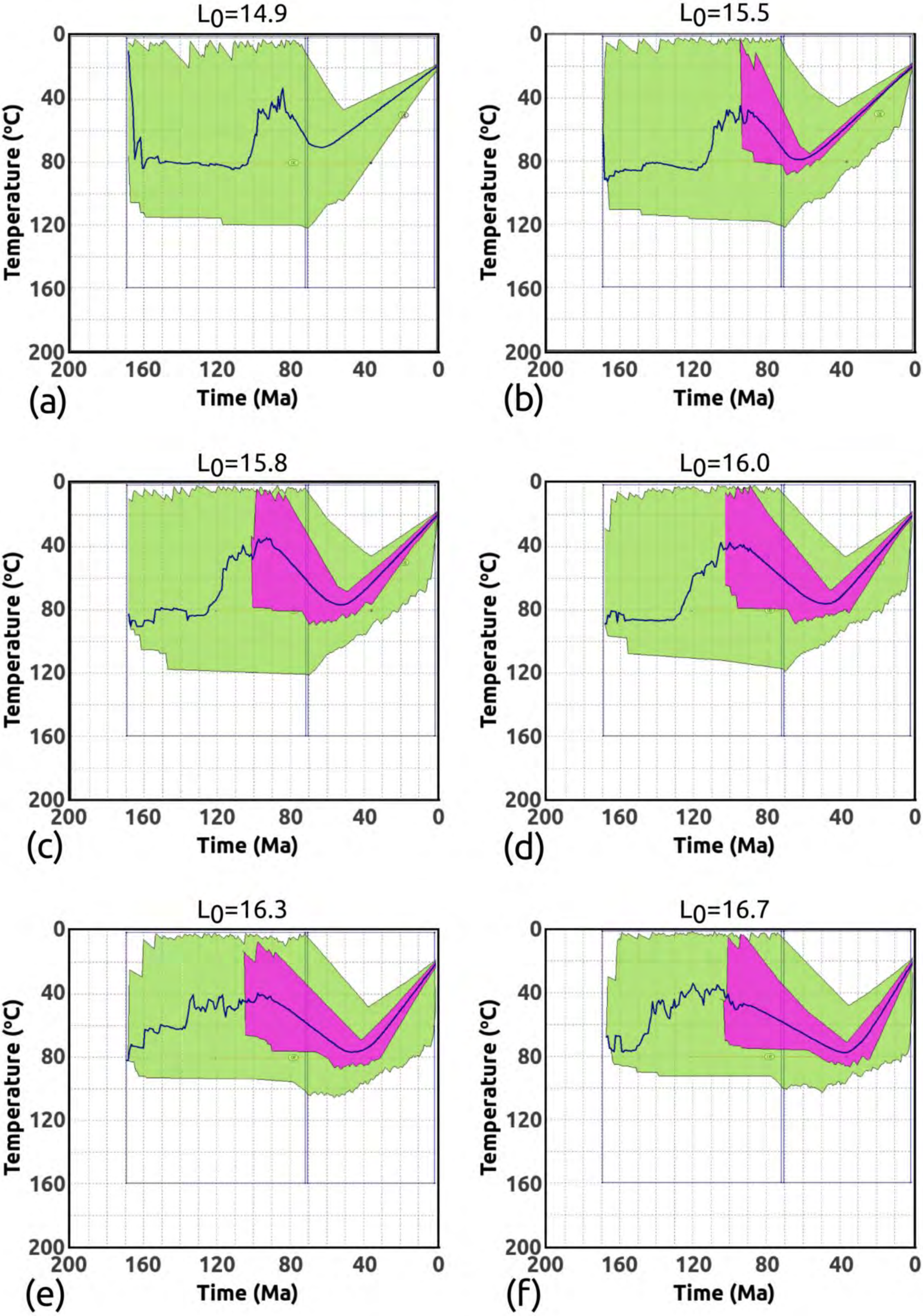
L_0=14.9
L_0=15.5
L_0=15.8
L_0=16.0
L_0=16.3
L_0=16.7
Temperature (°C)
Time (Ma)
(a)
(b)
(c)
(d)
(e)
(f)

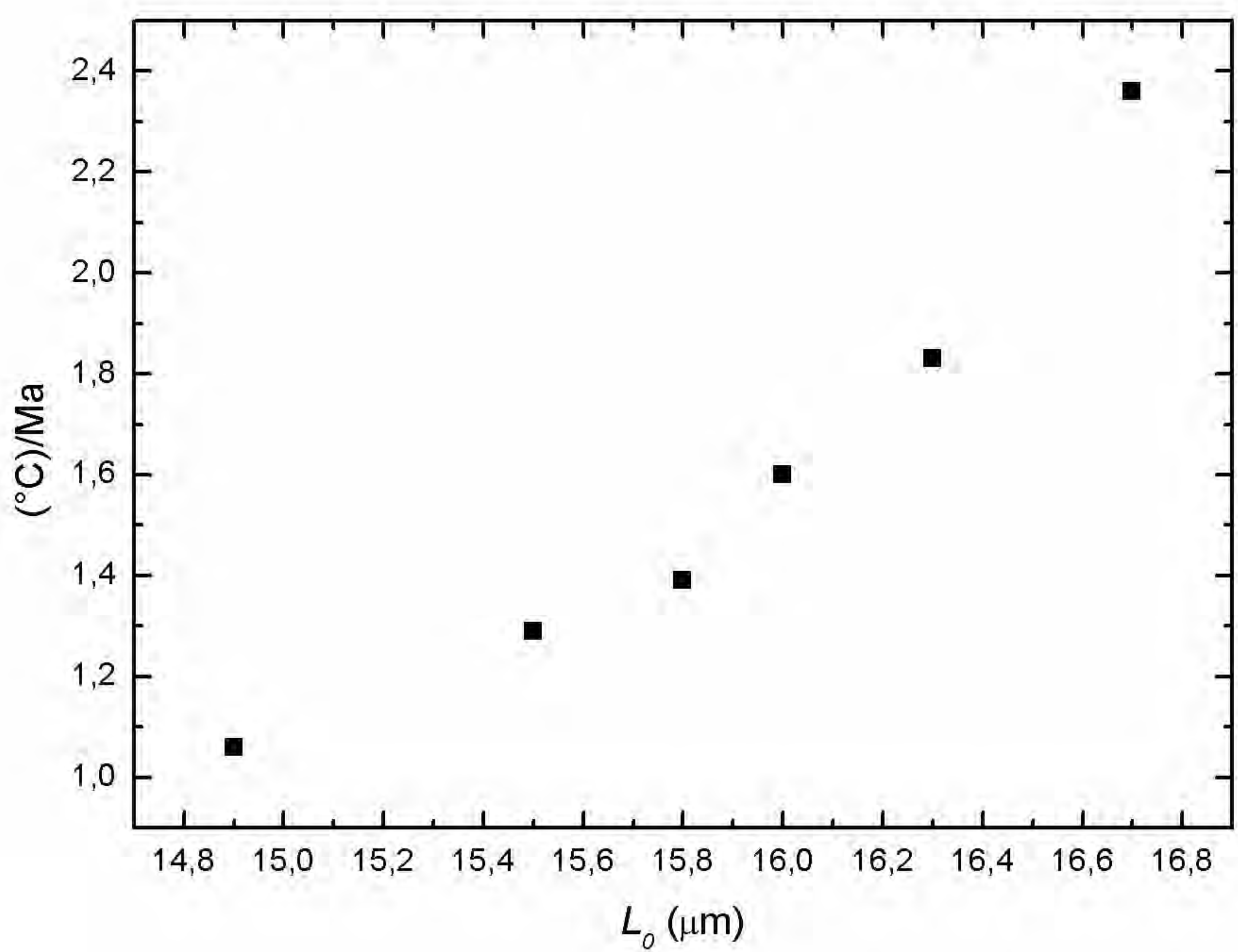
2,4
2,2
2,0
1,8
1,6
1,4
1,2
1,0
(°C)/Ma
14,8
15,0
15,2
15,4
15,6
15,8
16,0
16,2
16,4
16,6
16,8
L0 (μm)

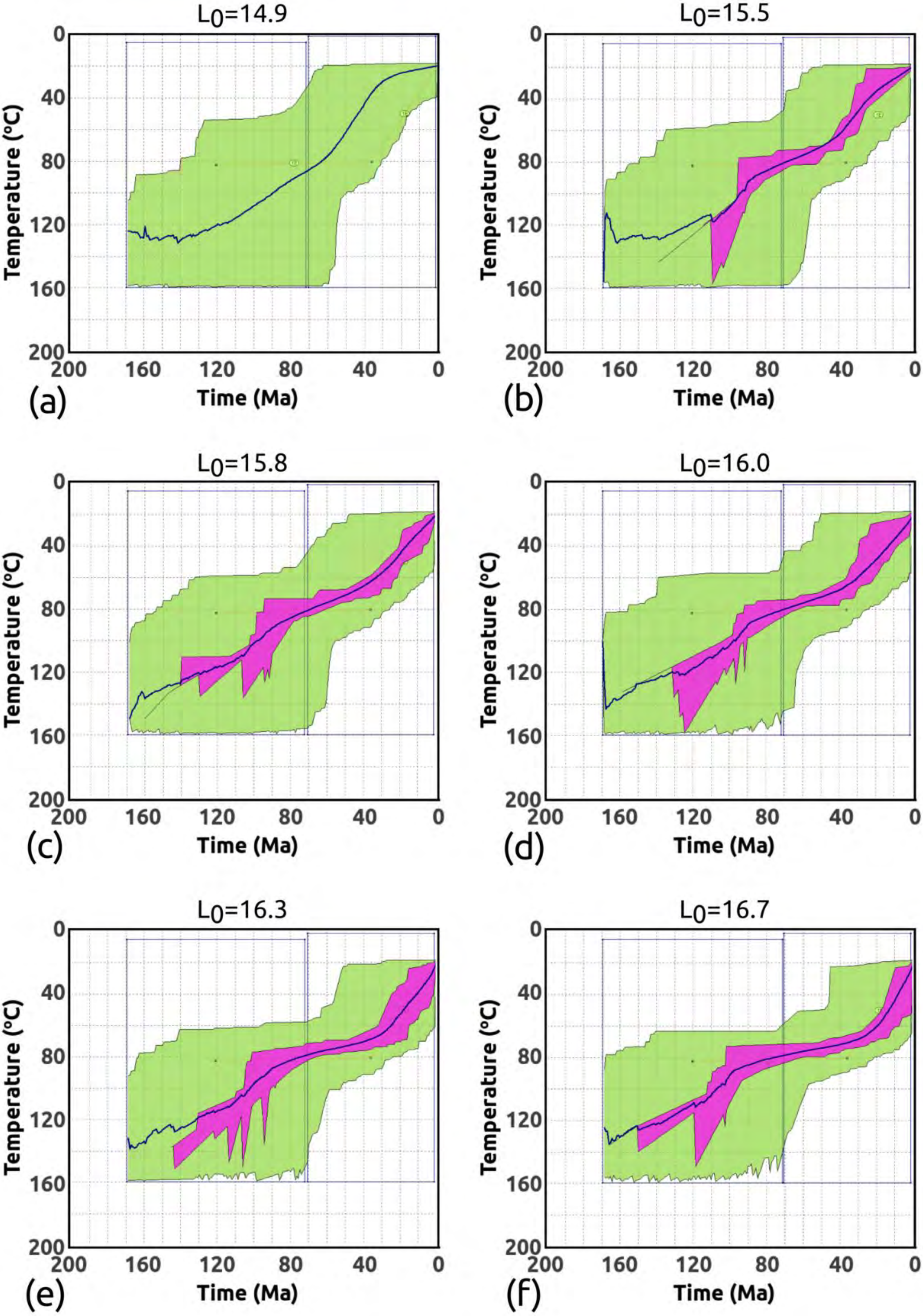
L0=14.9
L0=15.5
L0=15.8
L0=16.0
L0=16.3
L0=16.7
Temperature (ºC)
Time (Ma)
0
40
80
120
160
200
(a)
(b)
(c)
(d)
(e)
(f)

Table 1. Values of fission track densities and measured projected tracks.

N_{es} (f)	N_{is} (f)	$N_{is(es)}$ (f)	$N_{ed(is)}$ (f)	ρ_{ed}/ρ_{es} (±1σ)	$G=\rho_{ed}/\rho_{is}$ (±1σ)	ρ_{is}/ρ_{es} (±1σ)	$(\eta q)_{ed}$ (±1σ)	$(\eta q)_{is}$ (±1σ)	$[GQR]_{ed/is}$ (±1σ)
D-2 (Random orientation)									
2673 (42)	3199 (30)	2668 (42)	1897 (30)	1.00 (±0.03)	0.59 (±0.02)	1.68 (±0.04)	0.92 (±0.02)	0.94 (±0.01)	0.59 (±0.02)
D-3 (Random orientation)									
2275 (38)	2685 (26)	2320 (38)	1517 (26)	1.02 (±0.03)	0.57 (±0.02)	1.73 (±0.05)	0.93 (±0.02)	0.96 (±0.03)	0.59 (±0.02)
Mn-1 (Prismatic orientation)									
2446 (45)	3116 (30)	2497 (45)	1703 (30)	1.02 (±0.03)	0.55 (±0.02)	1.91 (±0.05)	0.93 (±0.02)	0.95 (±0.01)	0.59 (±0.02)
Mn-2									
2353 (38)	2944 (25)	1589 (38)	1588 (25)	0.68 (±0.02)	0.54 (±0.02)	1.90 (±0.05)	0.92 (±0.02)	0.92 (±0.01)	0.61 (±0.02)
TF-42 (Random orientation)									
1925 (45)	1979 (22)	1602 (45)	1055 (22)	0.83 (±0.03)	0.53 (±0.02)	2.10 (±0.07)	0.89 (±0.01)	1.00 (±0.05)	0.56 (±0.03)

N is the number of counted tracks in external surface (es), internal surface (is), external detector coupled to external surface (ed(es)), external detector coupled to internal surface (ed(is)), (f) is the number of counted fields, ρ are densities (using the same sub-index), ETA-q (ηq) values for muscovite (ed) and apatite (is). $[GQR]_{ed/is}$ is the product between $G(=2\pi/4\pi = 1/2)$, $Q = (\eta q)_{ed}/(\eta q)_{is}$ and the range deficit factor value, R. For Durango apatite, the R-value is 1.210±0.03 (as in Jonckheere, 2003), with L_0=16.28±0.21. For TF-42 R-value is 1.250±0.04 with L_0=15.71±0.28.

TABLE 2. Values of spontaneous and induced fission track densities using PM and EDM and ages obtained through EDM.

Sample	$(N_S)_{(EDM)}$	ρ_Sx10^6 (±1σ)	$N_{I(EDM)}$	$\rho_{I(EDM)}$ x10^6 (±1σ)	$N_{I(PM)}$	$\rho_{I(PM)}$x10^6 (±1σ)	L_0(±1σ)(N_C)	T_{EDM} (±1σ)	$g=\rho_{I(EDM)}/\rho_{I(PM)}$ (±1σ)	χ^2_ν (ν) (T_{EDM})
TF-5(1)*	107	0.14(±0.01)	139	0.17(±0.01)	202	0.33(±0.02)	15.5(±0.2)(54)	46.1(±6.3)	0.52(±0.06)	0.34 (20)
TF-9(1)‡	312	0.33(±0.02)	301	0.26(±0.01)	495	0.42(±0.02)	15.8(±0.2)(27)	70.9(±6.7)	0.62(±0.05)	1.51 (29)
TF-10(1)*	335	0.70(±0.04)	147	0.51(±0.04)	625	0.93(±0.04)	15.8(±0.1)(129)	76.6(±8.5)	0.55(±0.05)	1.96 (22)
TF-12(1)‡	329	0.33(±0.02)	370	0.44(±0.02)	638	0.78(±0.03)	16.0(±0.2)(96)	42.0(±3.8)	0.56(±0.04)	1.17 (26)
TF-17(2)*	177	0.34(±0.03)	54	0.21(±0.03)	347	0.43(±0.02)	15.4(±0.3)(28)	90.3(±14.7)	0.49(±0.07)	2.25 (16)
TF-21(3)*	130	0.58(±0.05)	232	0.78(±0.05)	307	1.55(±0.08)	15.4(±0.2)(26)	41.6(±5.0)	0.50(±0.04)	0.22 (15)
TF-30(2)*	394	0.41(±0.11)	253	0.56(±0.04)	586	0.91(±0.04)	---	41.0(±3.9)	0.62(±0.05)	0.31 (22)
TF-32(2)*	509	0.26(±0.01)	127	0.28(±0.02)	404	0.45(±0.02)	14.9(±0.4)(19)	51.9(±5.7)	0.62(±0.06)	0.44 (16)
						Average			**0.56±0.02**	

$N_S(N_I)$ are the numbers of counted spontaneous (induced) fission track for External Detector Method (EDM) and Population Method (PM); N_C are the number of induced horizontal confined fission-tracks; ρ_I are the induced densities for EDM and PM, the ratio $\rho_{I(EDM)}/\rho_{I(PM)}$ is the geometry factor for each sample, L_0 are the initial length of horizontal confined fission tracks and χ^2_ν is the reduced chi-square for the individual grain ages. These samples were presented previously in Tello et al. 2005. (1) Mantiqueira Mountain Range, (2) Mar Mountain Range, (3) Adjacent Areas.

*Gneiss

‡Granite